

**Electric instability in a two-dimensional electron gas system under high magnetic fields**Ching-Ping Lee,<sup>1</sup> C. C. Chi,<sup>1,2</sup> and Jeng-Chung Chen<sup>1,2</sup><sup>1</sup>*Department of Physics, National Tsing Hua University, Hsinchu 30013, Taiwan*<sup>2</sup>*Frontier Research Center on Fundamental and Applied Sciences of Matters, National Tsing Hua University, Hsinchu 30013, Taiwan*

(Received 28 April 2015; published 10 November 2015)

We present a study of electric instability in a two-dimensional electron gas system under high magnetic fields. As the applied dc electric current exceeds a threshold value  $I_{th}$ , we find that the longitudinal magnetoresistance  $R_{xx}$  fluctuates and exhibits negative differential resistivity (NDR). The observed instability occurs only in well-separated low-lying Landau levels (LLs) with a filling factor  $\nu \leq 2$ , and the onset of NDR can be described by the theory of Andreev *et al.* We find that  $I_{th}$  increases with increasing magnetic field  $B$  and the lattice temperature  $T_L$ . In contrast, NDR becomes more pronounced at higher  $B$ , but gradually diminishes with increasing  $T_L$ . Data analysis suggests that NDR is actuated by the suppression of  $R_{xx}$  with increasing electric field, which can be understood in terms of the capability of the spectral diffusion of electrons and of electron transfer to higher levels via inelastic inter-LLs scattering in the limit of one-occupied LL.

DOI: 10.1103/PhysRevB.92.195410

PACS number(s): 73.43.Qt, 73.63.Hs, 71.70.Di

Recent discoveries of various nonlinear phenomena in a two-dimensional electron gas (2DEG) system formed in a GaAs/AlGaAs heterostructure with high mobility in high magnetic fields have attracted considerable research interest [1]. These fascinating findings include microwave-induced resistance oscillations (MIRO) [2], zero-resistance states (ZRS) [3,4] for 2DEG samples subjected to intense microwave radiation, Hall field-induced resistance oscillations (HIRO) [5,6], and zero-differential resistance states (ZdRS) [7,8] in response to a strong dc electric field  $E$  excitation. These nonlinear states are accompanied intrinsically by electrical instability. For example, theories suggest that an ac  $E$  field induces a negative conductivity  $\sigma_{xx} < 0$  [9] and a nonlinear current density  $J$  electric field ( $J$ - $E$ ) relation [10]. Experimentally, negative differential resistance (NDR) is observed when an applied dc current  $I$  is above a threshold value  $I_{th}$  [7].

The nonlinear behaviors of 2DEG share several nonequilibrium features of NDR that are well known in bulk semiconductor materials, e.g., GaAs Gunn oscillator [11]. For bulk material, the decrease/increase of the resistance with the increase of  $E$  gives rise S-/N-shaped  $J$ - $E$  curves. Depending on material systems, NDR behaves differently in the presence of the magnetic field  $B$ ; for example, NDR is enhanced in bulk InSb [12], but is suppressed in GaAs semiconductor [13,14]. In bulk semiconductors different microscopic mechanisms have been proposed to understand various NDR behaviors [15–18].

The electric stability of a nonequilibrium 2DEG system under high  $B$  has been widely discussed in several theoretical papers [9,19,20]. Most of these theories are developed to explain ZRS phenomena [21]. Andreev *et al.* presented a physical model in Ref. [22] under the consideration of a local relation  $\mathbf{E} = \rho_{xx}(\mathbf{J}^2)\mathbf{J}$  together with the continuity and Poisson equation, and derived the following electric stability conditions:

$$\rho_{xx}(\mathbf{J}^2) \geq 0, \quad (1a)$$

$$\rho_{xx}(\mathbf{J}^2) + \xi \mathbf{J}^2 \geq 0, \quad (1b)$$

where  $\rho_{xx}$  is the longitudinal resistivity and  $\xi = 2\{d\rho_{xx}/[d(\mathbf{J}^2)]\}$ . The electric instability can be induced as either one of the conditions in Eq. (1) is violated. The theory of Andreev *et al.* is based on a phenomenological approach, and

is independent to the details of the microscopic mechanism. The instability criterion is in agreement with the recent observations of NDR on the maximum of Shubnikov–de Hass (SdH) oscillation of a nonequilibrium 2DEG system, where NDR is viewed as a precursor signal of ZdRS [7].

To date, most of the previous studies concentrated on nonequilibrium phenomena in high Landau levels (LLs) [1]. For example, MIRO can be found at the magnetic fields satisfying the condition  $\omega = n\omega_c$ , where  $\omega$  is the microwave frequency,  $\omega_c (= eB/m^*)$  is the cyclotron frequency,  $m^*$  is the effective mass of GaAs, and  $n = 1, 2, \dots$  [2]. Early experiments are carried out in  $B$  at which LLs are highly overlapped and the microwave frequency approximately ranges within  $20 < f < 150$  GHz. The ac frequency required in the regime of low LLs is out of reach in previous experiments, probably due to the difficulties to obtain strong radiation sources up to higher  $f$  to match  $\omega_c$ , e.g., in Ref. [2] two occupied LLs occur at  $B \sim 4.2$  T, giving  $\omega_c \sim 10.5$  THz ( $\hbar\omega_c \sim 6.9$  meV). Alternatively, dc-driven 2DEG provides a unique means to generate nonequilibrium electron distributions, and dc  $E$  field easily injects hot carriers with energy over 10 meV. Nevertheless, the features of electric instability in the low-LL regime can be overshadowed by the breakdown behaviors of the integer quantum Hall effect (IQHE) at low temperatures.

Our work aims to investigate the magnetoresistance instability driven by a dc electric field in low and well-separated LLs. This regime was less explored before and provides a unique condition for investigating the cyclotron dynamics among Landau levels [21,23]. We observe NDR in the condition of one-occupied LL at relatively high temperatures. The onset of NDR fits the stability conditions given in Eq. (1). We will show that the behaviors of NDR can be interpreted by energy distribution diffusion and inter-Landau-level transition driven by dc electric field.

Our samples are cleaved from a modulation-doped GaAs/Al<sub>0.3</sub>Ga<sub>0.7</sub>As single heterostructure crystals grown by molecular beam epitaxy. The device is fabricated on a wafer with an electron density of  $N_s = 3.1 \times 10^{11}$  cm<sup>-2</sup> and a mobility of  $\mu = 4.6 \times 10^5$  cm<sup>2</sup>/Vs at 1.5 K. The sample is a Hall bar with a width  $W = 100$   $\mu$ m and a distance  $L = 200$   $\mu$ m between voltage probes, as schematically shown in the

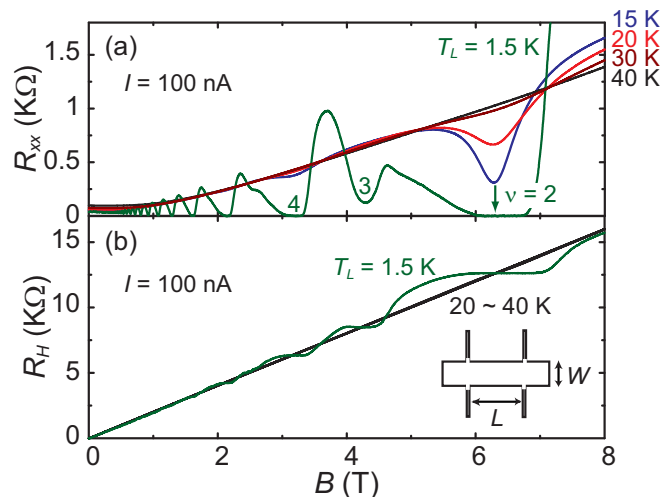


FIG. 1. (Color online) (a) Magnetic field dependence of longitudinal resistance  $R_{xx}$  for various lattice temperatures  $T_L$  and  $I = 100$  nA. (b) Magnetic field dependence of Hall resistance  $R_H$  for various lattice temperatures  $T_L$  and  $I = 100$  nA. The quantum Hall plateaus are thermally smeared out when  $T_L$  is higher than 20 K.  $R_H$  shows weak temperature dependence within  $T_L = 20$  to 40 K. The inset is a schematic of the device geometry.

inset in Fig. 1(b). The resistance is measured by transmitting square-wave current (17 Hz) alternating between  $I = 0$  and  $I_{SD}$ . We have ensured that the spatial distribution of the current or the electric field is homogeneous in the linear regime. For the details of experimental setup, refer to our previous publication [23]. All samples demonstrate consistent behavior. To save space, we only show representative data from one sample.

Figures 1(a) and 1(b) show the curves of longitudinal resistance  $R_{xx}$  and Hall resistance  $R_H$  versus  $B$  for various lattice temperatures  $T_L$  and  $I = 100$  nA, respectively, where  $R_{xx}(=V_{xx}/I)$  and  $R_H(=V_H/I)$ ,  $V_{xx}$  is the longitudinal voltage along the Hall bar and  $V_H$  is the Hall voltage. Clear Shubnikov–de Haas oscillations and integer quantum Hall effect (IQHE) are observed at  $T_L = 1.5$  K. The filling factor  $\nu \sim 2$  is at  $B = 6.36$  T. At higher  $T_L$ , the quantum Hall plateaus gradually vanish, as shown in Fig. 1(b). For  $\nu \sim 2$  state in  $T_L \sim 20$  to 40 K,  $R_{xx}$  apparently rises up and shows a dent. The measurements of nonequilibrium magnetotransport are performed at relatively high temperatures ( $T_L \geq 20$  K) at which IQHE are thermally smeared. Therefore, we can reasonably assume that the nonlinear properties of the quantum Hall breakdown have little effect on the current instability observed below.

Figures 2(a) and 2(b) show the dependence of  $V_{xx}$  on  $I$  for different  $T_L$  at  $B = 6.75$  T and different  $B$  at  $T_L = 20$  K, respectively. The  $V_{xx} - I$  curves are smooth, and weakly sublinear at sufficiently high  $I$  for  $B < 6.1$  T ( $\nu > 2$ ). When  $B$  is raised further,  $V_{xx}$  exhibits pronounced sublinearity with increasing  $I$ , and an evident drop  $\Delta V_{xx}$  as  $I$  exceeds a threshold value  $I_{th}$ . The unstable  $V_{xx}$  is attributed to the electric instability induced by NDR as  $I > I_{th}$ . Figures 2(c) and 2(d) show the dependence of the Hall voltage  $V_H$  versus  $I$  corresponding to Figs. 2(a) and 2(b), respectively. For approximately  $15$  K  $< T_L < 40$  K  $V_H$  shows weak  $T_L$  dependence, and exhibits smooth and weak superlinear

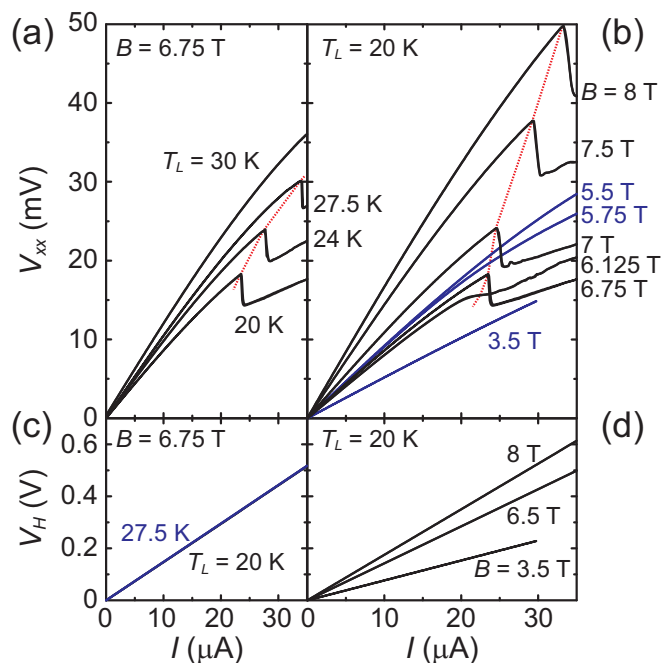


FIG. 2. (Color online) (a) Longitudinal voltage  $V_{xx}$  vs  $I$  for different  $T_L$  at  $B = 6.75$  T. The arrows mark where  $I = I_{th}$  above which electric instability takes place. The inset shows an exemplified trace of unstable features for  $I > I_{th}$  at  $T_L = 20$  K and  $B = 6.75$  T. (b)  $V_{xx}$  vs  $I$  for different  $B$  at  $T_L = 20$  K. (d) The Hall voltage  $V_H$  vs  $I$  traces at  $B = 6.75$  T and  $T_L = 20$  and 27.5 K. (e)  $V_H$  vs  $I$  traces at  $T_L = 20$  K for various  $B$ . Within  $T_L$  concerned,  $V_H$  exhibits weak temperature dependence, and nearly linear response with respect to  $I$  and  $B$  with no apparent anomaly.

behavior with  $I$ . Notably,  $I_{th}$  increases with increasing  $B$  and  $T_L$ , similar to the observations in the case of overlapped LLs [7]. Moreover,  $\Delta V_{xx}$  is larger at higher  $B$ , but decreases with increasing  $T_L$  and becomes indiscernible when  $T_L > 30$  K within the range of  $I$  applied. Figure 3 summarizes the changes of  $I_{th}$  and  $\Delta V_{xx}$  with  $I$  for different  $B$  and  $T_L$ .

This work focuses on NDR phenomena observed in the regime of well-separated low LLs, i.e.,  $3.5$  T  $< B < 8$  T corresponding to  $3.6 < \nu < 1.6$ , and at elevated temperatures  $20$  K  $< T_L < 30$  K. The spin-resolved QHS of  $\nu \sim 3$  is observed at  $T_L = 1.5$  K, but thermally smeared out as  $T_L > 5$  K, as shown in Fig. 1(b). Therefore, we only consider spin-degenerated LLs. We estimate the effective width of the level  $\Gamma \sim 0.26$  to  $1.2$  meV for  $T_L \sim 1.5$  to 30 K based on  $\Gamma = \hbar/\tau_q$ , where  $\tau_q$  is the quantum scattering time. Here, we evaluate  $\tau_q \sim 2.5$  ps by using the Shubnikov–de Haas (SdH) oscillations at  $T_L = 1.5$  K, and have  $\Gamma \sim 0.26$  meV. To obtain  $\Gamma$  at higher  $T_L$ , we assume  $\Gamma \propto \sqrt{T_L}$ , based on previous studies [24]. Our experiments cover a regime of  $\hbar\omega_c > k_B T_L > \Gamma$ .

Next, we focus on the detailed features of  $V_{xx}(I)$  evolving across NDR found in Fig. 2. We examine the differential resistance via  $r_{xx} = dV_{xx}/dI$ , and plot  $r_{xx}$  versus  $I$  in Fig. 4. Figures 4(a) and 4(b) show the  $r_{xx}$  versus  $I$  for different  $B$  at  $T_L = 20$  K and different  $T_L$  at  $B = 6.75$  T. In general,  $r_{xx}$  decreases sublinearly with the increase of  $I$ , consistent with those observed in high LLs case [25]. For the conditions at which NDR occurs,  $r_{xx}$  suddenly drops at  $I \sim I_{th}$  and subsequently become negative. Further increase  $I$  over  $I_{th}$ ,

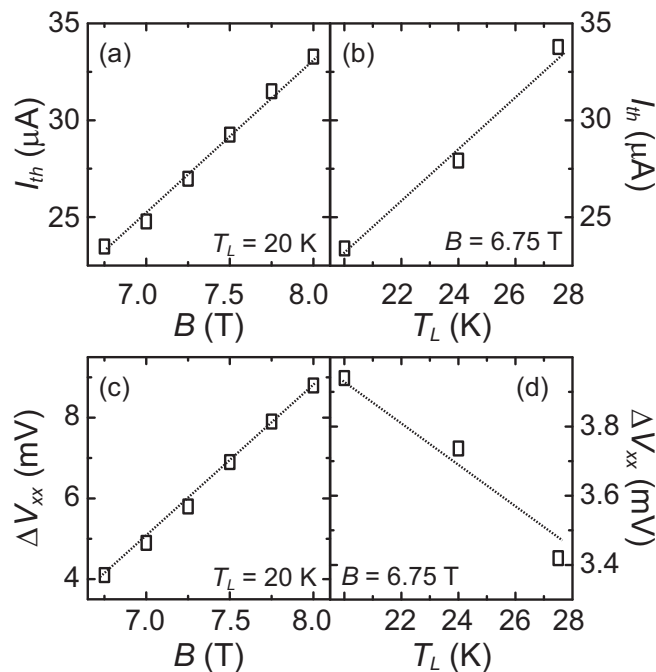


FIG. 3. Characteristics of NDR behaviors. (a)  $I_{th}$  vs  $B$  plot. (b)  $I_{th}$  vs  $T_L$  plot. (c)  $\Delta V_{xx}$  vs  $B$  plot. (d)  $\Delta V_{xx}$  vs  $T_L$  plot.

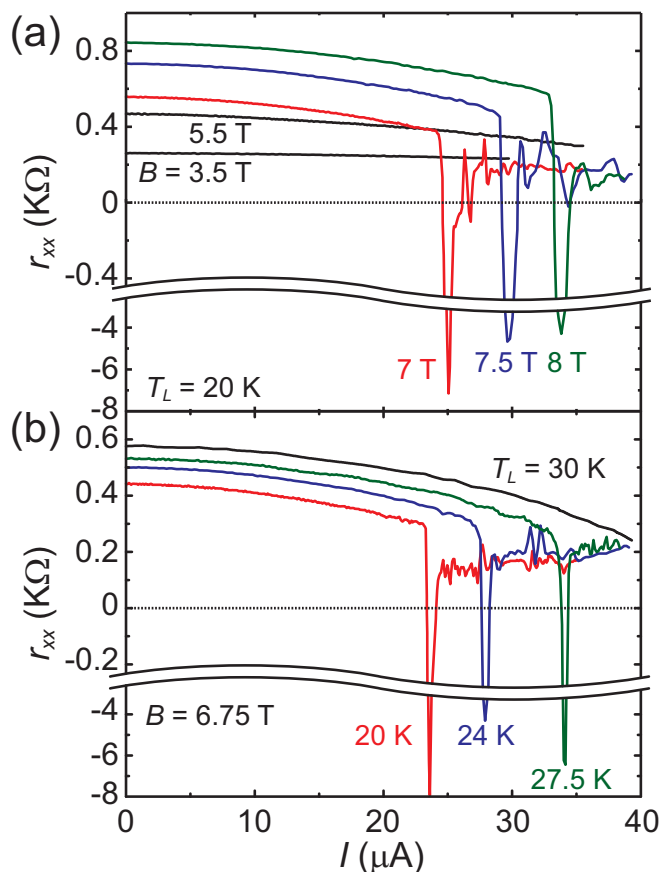


FIG. 4. (Color online) (a) Longitudinal differential resistivity  $r_{xx}$  vs  $I$  for various  $B$  at  $T_L = 20$  K. (b) Longitudinal differential resistivity  $r_{xx}$  vs  $I$  for various  $T_L$  at  $B = 6.75$  T.

$r_{xx}$  restores to a positive value in a metastable state with irregular and reproducible fluctuations. Distinctly, different to a previous report [7], we do not find ZdRS in our experiments.

To compare our results with Eq. (1), we note that  $R_{xx}$  is always positive in our measurements. Therefore, the electric stability is governed by Eq. (1b). It has been shown that Eq. (1b) can be rewritten as  $\rho_{xx}^d \geq 0$  [7], where  $\rho_{xx}^d = dE_x/dJ_x$  is the longitudinal differential resistivity,  $E_x$  is longitudinal electric field, and  $J_x$  is longitudinal current. It is important to note that the basic for this correlation is resulted from the  $J^2$  dependence of  $\rho_{xx}$ . Experimentally,  $E_x$  and  $J_x$  can be derived by the relations  $E_x = V_{xx}/L$  and  $J_x = I/W$ , respectively. We obtain  $r_{xx} = \gamma \rho_{xx}^d$ , where  $\gamma (=L/W)$  is a factor to account geometric size of the device, and  $\gamma = 2$  in our case. Consequently, the occurrence of negative  $r_{xx}$  as a sign of electric instability is in agreement with the prediction of Eq. (1b). We verify that Eq. (1) can be used as the electric stability conditions for nonequilibrium 2DEG, and NDR induces the electric instability regardless the presence of  $B$ .

Next, we turn to discuss the mechanism responsible for NDR. Our previous analysis suggests that NDR is strongly correlated to a reduction in  $r_{xx}$  with increasing  $I$ , i.e., the decrease of  $\rho_{xx}$  with increasing  $E$ . It can be seen from Fig. 1 that simple electron heating effect cannot explain the suppression of  $\rho_{xx}$  observed over a broad range of magnetic fields and temperatures [26]. Experimentally, in the case of 2DEG with overlapped LLs,  $R_{xx}$  has been reported to be strongly suppressed with increases in  $E$ . The reduction in resistance even survives at high temperatures for  $k_B T_L > \hbar \omega_c$  [25]. Theoretically, the nonlinearity of  $\rho_{xx}(E)$  can be attributed to the formation of the nonequilibrium distribution function [21,26] and the inelastic scattering among LLs [5,27]. The external  $E$  accelerates electrons and facilitates an inelastic intra- or inter-LLs scattering [26]. In strong magnetic fields, this scattering process leads electrons to diffuse in the direction of  $\mathbf{E}$  [23]: Moreover, to conserve the total energy, the spatial diffusion can be translated into the diffusion in energy space with a diffusion coefficient  $(eE)^2 D_B(\epsilon)$  where  $D_B(\epsilon) = v_F^2 / 2\omega_c^2 \tau_{tr}$ ,  $v_F$  is the Fermi velocity, and  $\tau_{tr}$  is the transport scattering times. This process leads to a nontrivial change  $\delta f$  in the distribution function modulated by the density of state [21]. It is theoretically shown that  $\rho_{xx}$  decreases with increasing  $E$ , and the reduced amount  $\Delta \rho_{xx}$  (through  $\Delta \rho_{xx} \sim \rho_H^2 \Delta \sigma_{xx}$ ) is governed by a dimensionless parameter  $Q_{dc}$ :

$$Q_{dc} = \frac{2\tau_{in}}{\tau_{tr}} \left( \frac{eE v_F}{\omega_c} \right)^2 \left( \frac{\pi}{\hbar \omega_c} \right)^2. \quad (2)$$

Here,  $\tau_{in}$  is the inelastic scattering time and scales with  $T_L$  as  $\tau_{in} \propto 1/T_L^2$ . Under a high magnetic field, the spectrum diffusion capability is blocked by the larger LL gaps, manifesting as a decrease in  $D_B$ ; in contrast, higher  $T_L$  renders a smaller  $\tau_{in}$ . The overall effect of increasing either  $B$  or  $T_L$  is to make  $Q_{dc}$  smaller [see Eq. (2)]. Therefore, to retain  $\Delta \rho_{xx}$  higher  $E$  needs to be applied. This explains why  $I_{th}$  increases with the increase of  $B$  or  $T_L$ , as shown in Figs. 3(a) and 3(b). Nevertheless, increasing  $B$  and  $T_L$  produces an inverse effect on the electric instability: NDR phenomena gradually become extinct as  $T_L$  increases, but become more pronounced at higher  $B$  [see Figs. 3(c) and 3(d)]. To understand this difference, we

should consider that as the applied current increases over  $I_{th}$  the 2DEG system undergoes a phase transition from a stable high-conductivity state to another low-conductivity state. This transition, particularly for the case of well-separated low LLs, is likely accompanied by the inter-LL scattering process, and this inter-LL transition channels the injection energy into higher LL by an amount that scales with  $\hbar\omega_c$ . In a strong dc  $E$  field, the inter-LL transition becomes more efficient and the transmitted energy increases with  $B$ ; therefore, the  $\Delta V_{xx}$  observed at  $I \sim I_{th}$  is larger at higher  $B$ . In contrast, raising  $T_L$  enhances the loss rate of the injection energy into the lattice due to the smaller  $\tau_{in}$ , and the inter-LL transition is demoted. Hence,  $\Delta V_{xx}$  diminishes with increasing  $T_L$ . On the other hand,  $\tau_{in}$  originating from the impurity scattering also decreases with decreasing  $B$ . Likewise, NDR is less visible at lower  $B$ . We note that  $\tau_{in} \sim 400$  ps at  $T_L = 2$  K in our sample, which is one order of magnitude smaller than that in Refs. [7,26]. This may explain why we are unable to observe NDR in the overlapped LLs regime in our experiments.

In summary, electric instability is observed in 2DEG systems with one-occupied LL when the current passing through the Hall-bar samples exceeds a threshold value  $I_{th}$  at relatively high temperatures  $T_L \sim 17\text{--}35$  K. The longitudinal resistance  $R_{xx}$  decreases with increasing current  $I$ . As  $I$  exceeds a threshold value  $I_{th}$ ,  $R_{xx}$  drops and exhibits irregular fluctuations. In the vicinity of  $I_{th}$ , NDR is found. The onset of  $I_{th}$  fits to a stability condition proposed by Andreev *et al.* [22]. The value of  $I_{th}$  increases with increasing  $B$  and  $T_L$ . In contrast, NDR becomes more pronounced at higher  $B$ , but gradually diminishes with increasing  $T_L$ . We attribute the behaviors of NDR to an electric-field-induced nontrivial electron distribution function and the effects of the inter-LL transition in a high magnetic field.

We thank K.-T. Lin for experimental assistance. This project is supported by Ministry of Science and Technology, Taiwan under Grant No. MOST 101-2628-M-007-002-MY3, Taiwan.

- 
- [1] I. A. Dmitriev, A. D. Mirlin, D. G. Polyakov, and M. A. Zudov, *Rev. Mod. Phys.* **84**, 1709 (2012).
- [2] M. A. Zudov, R. R. Du, J. A. Simmons, and J. L. Reno, *Phys. Rev. B* **64**, 201311(R) (2001).
- [3] R. G. Mani, J. H. Smet, K. von Klitzing, V. Narayanamurti, W. B. Johnson, and V. Umansky, *Nature (London)* **420**, 646 (2002).
- [4] M. A. Zudov, R. R. Du, L. N. Pfeiffer, and K. W. West, *Phys. Rev. Lett.* **90**, 046807 (2003).
- [5] C. L. Yang, J. Zhang, R. R. Du, J. A. Simmons, and J. L. Reno, *Phys. Rev. Lett.* **89**, 076801 (2002).
- [6] A. A. Bykov, J.-q. Zhang, S. Vitkalov, A. K. Kalagin, and A. K. Bakarov, *Phys. Rev. B* **72**, 245307 (2005).
- [7] A. A. Bykov, J.-q. Zhang, S. Vitkalov, A. K. Kalagin, and A. K. Bakarov, *Phys. Rev. Lett.* **99**, 116801 (2007).
- [8] A. T. Hatke, H.-S. Chiang, M. A. Zudov, L. N. Pfeiffer, and K. W. West, *Phys. Rev. B* **82**, 041304 (2010).
- [9] A. C. Durst, S. Sachdev, N. Read, and S. M. Girvin, *Phys. Rev. Lett.* **91**, 086803 (2003).
- [10] F. S. Bergeret, B. Huckestein, and A. F. Volkov, *Phys. Rev. B* **67**, 241303(R) (2003).
- [11] B. K. Ridley, *Proc. Phys. Soc.* **82**, 954 (1963).
- [12] V. N. Bogomolov, S. G. Shulman, A. G. Aronov, and G. E. Pikus, *Zh. Eksp. Teor. Fiz. Pis. Red.* **5**, 212 (1967) [*JETP Lett.* **5**, 169 (1967)].
- [13] M. E. Levinshstein, T. V. Lvova, D. N. Nasledov, and M. S. Shur, *Phys. Status Solidi A* **1**, 177 (1970).
- [14] A. Patanè, A. Ignatov, D. Fowler, O. Makarovsky, L. Eaves, L. Geelhaar, and H. Riechert, *Phys. Rev. B* **72**, 033312 (2005).
- [15] R. F. Kazarinov and V. G. Skobov, *Zh. Eksp. Teor. Fiz.* **44**, 1368 (1963) [*Sov. Phys.-JETP* **17**, 921 (1963)].
- [16] F. G. Bass, *Zh. Eksp. Teor. Fiz.* **48**, 275 (1965) [*Sov. Phys.-JETP* **21**, 181 (1965)].
- [17] V. F. Elesin, *Zh. Eksp. Teor. Fiz.* **55**, 792 (1969) [*Sov. Phys.-JETP* **28**, 410 (1969)].
- [18] A. D. Gladun and V. I. Ryzhii, *Zh. Eksp. Teor. Fiz.* **57**, 978 (1970) [*Sov. Phys.-JETP* **30**, 534 (1970)].
- [19] J. Shi and X. C. Xie, *Phys. Rev. Lett.* **91**, 086801 (2003).
- [20] A. Kunold and M. Torres, *Phys. Rev. B* **80**, 205314 (2009).
- [21] I. A. Dmitriev, M. G. Vavilov, I. L. Aleiner, A. D. Mirlin, and D. G. Polyakov, *Phys. Rev. B* **71**, 115316 (2005).
- [22] A. V. Andreev, I. L. Aleiner, and A. J. Millis, *Phys. Rev. Lett.* **91**, 056803 (2003).
- [23] J. C. Chen, Y. Tsai, Y. Lin, T. Ueda, and S. Komiyama, *Phys. Rev. B* **79**, 075308 (2009).
- [24] M. P. Chaubey and M. Singh, *Phys. Rev. B* **34**, 2385 (1986).
- [25] J.-q. Zhang, S. Vitkalov, A. A. Bykov, A. K. Kalagin, and A. K. Bakarov, *Phys. Rev. B* **75**, 081305(R) (2007).
- [26] J. Q. Zhang, S. Vitkalov, and A. A. Bykov, *Phys. Rev. B* **80**, 045310 (2009).
- [27] W. Zhang, M. A. Zudov, L. N. Pfeiffer, and K. W. West, *Phys. Rev. Lett.* **100**, 036805 (2008).